2014 IEEE International Conference on Robotics & Automation (ICRA)
Hong Kong Convention and Exhibition Center
May 31 - June 7, 2014. Hong Kong, China

Automated Capsulorhexis Based on a Hybrid Magnetic-Mechanical Actuation System

Franziska Ullrich[1], Simone Schuerle[1], Roel Pieters[1], Avraham Dishy[2], Stephan Michels[3] and Bradley J. Nelson[1]

***Abstract*— This paper presents a hybrid magnetic-mechanical manipulation system for automated capsulorhexis utilizing a flexible catheter with a sharp edge magnetic tip. Vision based closed loop control is implemented to guide the tip on a circular path in the anterior eye segment. A continuous motion with high repeatability is achieved. The system shows the first catheter-based application of the electromagnetic manipulation system, OctoMag, for fast and safe ophthalmic surgery that potentially reduces the risk of complications and improves precision.**

I. INTRODUCTION

Cataracts are the leading cause of blindness and accounts for 51% of world visual disability [1]. In 2010 17.11% of the U.S. population over 40 years of age were affected by this visual impairment [2]. Cataracts are often associated and increasing with old age. The disease describes the gradual opacification of the crystalline lens and is clinically graded according to color, opacity and amount of cortical, nuclear and posterior subcapsular cataract. It is routinely treated by surgery, where corneal incisions are made at the limbus to allow for insertion of instruments into the aqueous anterior chamber of the eye. Subsequently, a bent needle (cystotome) or a special forceps is used to create a circular hole in the anterior lens capsule, a procedure known as continuous circular capsulorhexis, illustrated in Figure 1. The lens is then hydrated to delineate the capsule from the cortex, followed by breaking the lens into fragments using phacoemulsification and subsequent removal of the fragments from the capsular bag. After inflation of the capsular bag with a viscoelastic fluid, an artificial foldable intraocular lens (IOL) is injected into the capsular bag. The size, shape and location of the opening in the anterior lens capsule are crucial. No tears should occur in the lens capsule during or after surgery as it could prevent implanting the IOL in the capsular bag [3]. It has been shown that posterior capsular opacification (PCO) can be prevented by opening the anterior lens capsule circularly in the centre of the lens with a diameter between 5 mm and 7 mm, so that the anterior lens capsule can overlap with the IOL optic surface and stabilize it [4], [5]. The ideal capsulorhexis edge should be continuous to allow for highest strength [3] and has been suggested to overlap with the IOL optics by 0.5 mm [6]. Achieving an intact, centrally located,

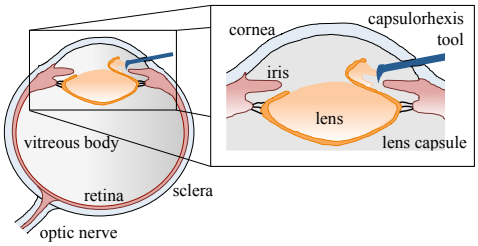

Fig. 1. The basic anatomy of the human eye and a more detailed view of the anterior section of the eye. Capsulorhexis is one of the key steps in cataract surgery and describes the process of creating a circular hole in the lens capsule.

and perfectly circular capsulorhexis is crucial to the safety and best outcome of cataract surgery. This surgery requires high precision and is technically difficult to learn as the delicate structures of the anterior eye are under constant risk of damage due to the rigid instruments used by the ophthalmologist and a lack of precision arising from the limits of human force perception [7], [8].

Several robotic platforms have been developed to assist in ophthalmic surgery for decreasing the risk of damage to the delicate structures of the eye and for faster recovery of the patient, and thus, making procedures safer and easier. Teleoperation systems [9]–[11], cooperatively controlled hand-over-hand system [12] and freehand active tremor-filtering systems [13] have been suggested to aid in eye surgery. Moreover, recent emerging technologies have paved the way for flexible surgical tools, such as magnetically guided catheters to increase stability, precision and minimize the risk of perforation of tissue [14]–[16]. Systems utilizing permanent magnets [17] or electromagnets [18], [19] guide a magnetic catheter precisely during medical procedures.

In this paper we propose a system for automated minimally invasive capsulorhexis utilizing a flexible catheter with a customized curved needle as end-effector. This tool is used to circumscribe a circular path inside the aqueous chamber of the eye to create a well-defined capsulorhexis in the anterior lens capsule in a continuous movement. The catheter is guided with a hybrid magnetic-mechanical actuation system consisting of a linear piezoelectric actuator (PEA) that controls the longitudinal motion of the tip while the lateral movement is controlled by an electromagnetic manipulation system, the OctoMag.

[1]Institute for Robotics and Intelligent Systems (IRIS), ETH Zurich, Tannenstrasse 3, 8092 Zurich, Switzerland bnelson@ethz.ch
[2]Department of Ophthalmology, Kantonsspital Aarau, Tellstrasse, 5001 Aarau, Switzerland
[3]Department of Ophthalmology,Triemli Hospital Zurich, Birmensdorferstrasse 497, 8063 Zurich, Switzerland

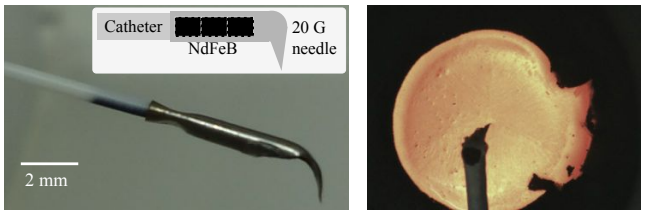

(a) (b)

Fig. 2. a) The magnetic tool for capsulorhexis consists of a 2 Fr PUR catheter with a bent 20 gauge injection needle. b) The tool in front of a porcine lens for size comparison.

II. EXPERIMENTAL SETUP

A. Magnetic Catheter

The surgical instrument used for capsulorhexis consists of a conventional polyurethane (PUR) catheter (2 Fr, Vygon, Aachen, Germany) with an outer diameter of 0.6 mm and an inner diameter of 0.3 mm. The customized end-effector consists of the bent tip of a 20 gauge injection needle and is attached to one end of the PUR catheter. Three cylindrical Neodymimum-Iron-Boron (NdFeB) magnets (diameter 0.5 mm and length 1.0 mm) with a combined magnetic volume of 0.589 mm^3 are inserted into the needle tip without separation. The magnetic tool is illustrated in Figure 2.

B. Piezoelectric Actuator

Movements of the catheter tip in longitudinal direction are governed by a linear cartesian piezoelectric stepping actuator (SLC-1740, SmarAct GmbH, Oldenburg, Germany) with only one active direction. This manipulator consists of three linear positioners that each allow for 21 mm of travel and are mounted on a base plate with an integrated sensor module to perform closed loop positioning control with a sensor resolution of 50 nm, whereas the flexibility of the catheter might reduce the positioning precision and accuracy of the full system. The linear actuator is activated with customized software written in LabView (National Instruments, Austin, TX, US). Prior to execution, a file is generated with a MATLAB simulation, explained in section III-B, that describes the desired path with preset spatial step size. The software initializes the positioner and feeds the desired position values to the PEA controller, such that the manipulator moves each step before waiting a determined time t_{sleep} in [ms]. Hence, the longitudinal velocity of the catheter is regulated by the PEA. The actuator allows for maximum velocity of 13 mm/s. The advancing velocity of the catheter was recorded with a vision based blob tracker at different spatial step sizes and with various sleep times, as illustrated in Figure 3.

C. Magnetic Manipulation System

The OctoMag was introduced by Kummer et al. [20] in 2010. A second version was built in 2011, shown in Figure 4a), that is movable and mechanically more stable than the prototype. It also allows for slightly higher magnetic fields of up to 40 mT and magnetic field gradients of 1 T/m. The OctoMag has been shown to successfully guide untethered microrobots during minimally invasive surgery in the posterior eye segment in *ex vivo* and *in vivo* applications [21], [22]. The system consists of eight electromagnetic coils with soft-magnetic cores in a hemispherical arrangement. The central workspace created by this arrangement is $20 \times 20 \times 20$ mm, and by adjusting the currents within the electromagnetic coils the magnetic fields and magnetic gradients can be controlled, guiding magnetic devices with high spatial precision [23]. The lateral motion of the magnetic needle tip of the catheter is observed through a CCD camera at 120 Hz (Grasshopper 03K2C-C, Pointgrey, BC, Canada) and is visually guided in the horizontal plane by a controller, described in section III, through the OctoMag workspace. The complete system consisting of OctoMag and PEA that is utilized for flexible catheter control for capsulorhexis is sketched in Figure 4b). It should be noted, that the OctoMag is capable of 5 degree-of-freedom control, and hence is over actuated for the application described in this work as only lateral motion of the catheter and its pitch are controlled.

III. CONTROL

A. Governing Equations

The catheter tip is equipped with three cylindrical NeFeB magnets with a diameter of 0.5 mm and length 1 mm with total magnetization $\mathbf{M}$ in $[\mathrm{A/m}]$. It is assumed that the magnetization is largest along the longitudinal direction of the catheter while magnetization in the radial direction can be neglected. When the catheter tip is positioned within the workspace, it is exposed to an external magnetic field $\mathbf{H}$ in $[\mathrm{A/m}]$, generated by the OctoMag. The magnetic flux density $\mathbf{B}$ in $[\mathrm{T}]$ is derived by $\mathbf{B}= \mu_0\mathbf{H}$, where $\mu_0= 4\pi \times 10^{-7}$ Tm/A is the permeability of vacuum. When an external magnetic field is generated, the magnetic torque per volume $\mathbf{T} = \mathbf{M} \times \mathbf{B}$ in $[\mathrm{N/m^2}]$ aligns the magnetic catheter tip with the applied field $\mathbf{B}$. As no electric current flows through the workspace occupied by the catheter tip, $\nabla \times \mathbf{B} = 0$, and

$$\mathbf{F} = (\nabla \cdot \mathbf{B})^T \mathbf{M} = \left[\frac{\partial \mathbf{B}}{\partial x} \quad \frac{\partial \mathbf{B}}{\partial y} \quad \frac{\partial \mathbf{B}}{\partial z} \right]^T \mathbf{M} \qquad (1)$$

the magnetic force per volume in $[\mathrm{N/m^3}]$ can be written as $\mathbf{F} = (\mathbf{M} \cdot \nabla)\mathbf{B}$. The OctoMag consists of eight electromagnets

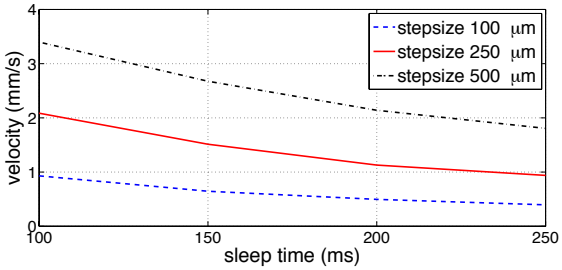

Fig. 3. Velocity of the catheter tip in [mm/s] as a result of sleep time in [ms] and step size in [µm] of the PEA as measured with visual tracking.

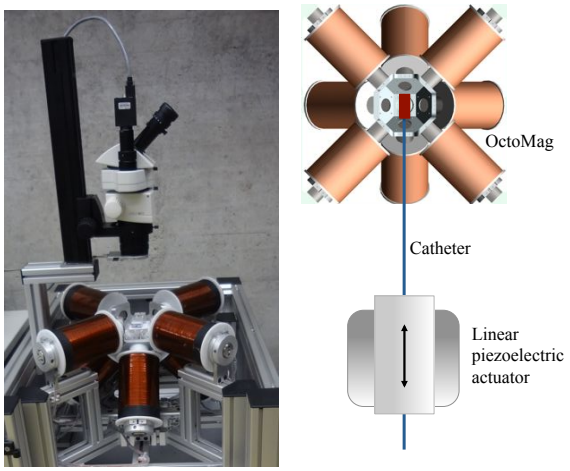

(a) (b)

Fig. 4. a) The magnetic manipulation system OctoMag including eight electromagnetic coils. The second version is mechanically more stable and can generate slightly higher magnetic fields than the prototype, which was introduced in [20]. b) The hybrid magnetic-mechanical system with a linear piezoelectric actuator (PEA) and the magnetic manipulation system OctoMag as seen from above.

that each create a magnetic field, which can be precomputed. The magnetic field at a point $\mathbf{P}$ in the workspace due to activating a single electromagnet e is given as $\mathbf{B}_e(\mathbf{P}) = \tilde{\mathbf{B}}_\mathbf{e}(\mathbf{P})i_e$, where $\tilde{\mathbf{B}}_\mathbf{e}$ is the unit contribution and i_e is the current in coil e, respectively. By imposing the fields generated by all electromagnets at a point $\mathbf{P}$ in the workspace the field at this point is derived as

$$\mathbf{B}(\mathbf{P}) = \sum_{e=1}^{8} \tilde{\mathbf{B}}_e(\mathbf{P})i_e = \mathscr{B}(\mathbf{P})I \tag{2}$$

where vector I holds the currents in each coil and $\mathscr{B}(\mathbf{P})$ is a 3×8 unit field contribution matrix that can be analytically calculated online or interpolated from precomputed or measured points. Magnetic force and torque applied to the catheter tip can be expressed as

$$\begin{bmatrix} \mathbf{T} \\ \mathbf{F} \end{bmatrix} = \begin{bmatrix} Sk(\hat{\mathbf{M}})\mathscr{B}(\mathbf{P}) \\ \hat{\mathbf{M}}^T \frac{\partial \mathscr{B}}{\partial x}(\mathbf{P}) \\ \hat{\mathbf{M}}^T \frac{\partial \mathscr{B}}{\partial y}(\mathbf{P}) \\ \hat{\mathbf{M}}^T \frac{\partial \mathscr{B}}{\partial z}(\mathbf{P}) \end{bmatrix} \begin{bmatrix} i_1 \\ \vdots \\ i_8 \end{bmatrix} = \mathscr{A}(\hat{\mathbf{M}}, \mathbf{P})I \tag{3}$$

where the eight electromagnet currents are mapped to magnetic force and torque through the 6×8 actuation matrix $\mathscr{A}(\hat{\mathbf{M}}, \mathbf{P})$ and $Sk(\hat{\mathbf{M}})$ is the skew-symmetric matrix form of $\hat{\mathbf{M}}$. To remove any dependencies on the magnetic properties of the catheter tip material the magnetization $\mathbf{M}$ is normalized with respect to the volume magnetization of the material in $[\mathrm{Am}^2]$ and written as $\hat{\mathbf{M}}$. For a desired torque/force vector to manipulate the magnetic catheter tip, the required currents in the electromagnets can be found by using the pseudoinverse of $\mathscr{A}$

$$I = \mathscr{A}(\hat{\mathbf{M}}, \mathbf{P})^\dagger \begin{bmatrix} \mathbf{T_{des}} \\ \mathbf{F_{des}} \end{bmatrix} \tag{4}$$

A detailed mathematical model describing the OctoMag can be found in [24].

With the current system the applied torques are much more effective on the motion of the magnetic catheter tip than applied forces. The forces, derived from magnetic gradients, are too weak to actively pull and push the long catheter body and its tip. Therefore, the longitudinal motion of the catheter is governed by the PEA while the catheter orientation is controlled by applying magnetic torques. In order to cut through the capsular bag of the lens during capsulorhexis, forces in vertical direction can be applied. The catheter is controlled in an aqueous environment to model real conditions in the aqueous chamber of the anterior eye.

B. Kinematic model

To simulate the control of the magnetic catheter tip on a circular path, a kinematic model is derived in MATLAB that calculates the motion parameters of the catheter. It is assumed that there is zero curvature along the length of the catheter, i.e. that it is a straight line at all times. The user defines the anchor point $\mathbf{A}$ of the catheter, at which a shaft restricts the lateral motion of the catheter, corresponding to the insertion point in a physical procedure. To approach the circular path, described by points $\mathbf{K^j} = (x_j, y_j)$, the catheter travels a predefined longitudinal distance of length L, as illustrated in Figure 5. The length l_j of the catheter at point $\mathbf{K^j}$ is given by $l_j = \|\overline{\mathbf{AK^j}}\|$ whereas the angle of orientation of the catheter tip α_j is given by

$$\alpha_j = \arcsin\left(\frac{x_j}{\|\overline{\mathbf{AK^j}}\|}\right) \tag{5}$$

Figure 6 illustrates the parameters α_j and l_j versus time. In this example, a circle with radius $R = 5$ mm is circumscribed by the simulated catheter tip within a time of 10 s where distance $L = 3$ mm.

C. Closed Loop Control

For model based closed loop control the catheter tip is visually tracked at all times using a blob tracking algorithm,

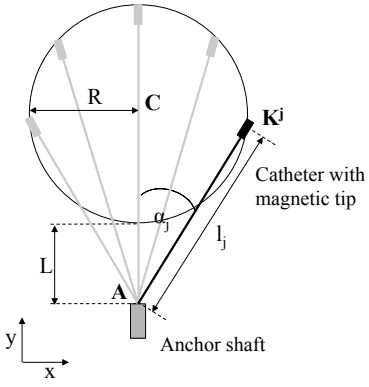

Fig. 5. The catheter is anchored at the anchor shaft $\mathbf{A}$, it describes a circular path with radius R with parameters l_j and α_j. The length of the catheter l_j is governed by the PEA while orientation α_j is controlled by the OctoMag.

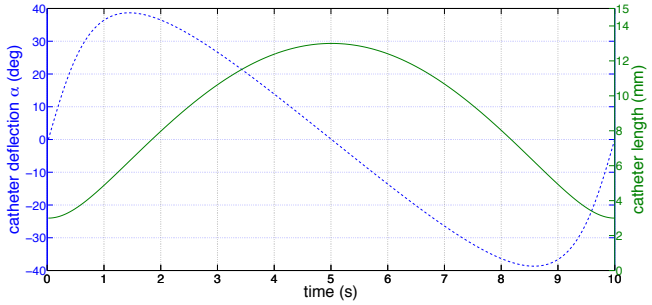

Fig. 6. The MATLAB simulation derives the required length l_j and orientation α_j of the catheter at any given point K_j at a time in [s] on the circular path with radius R. In this example, R =5 mm, L =3 mm.

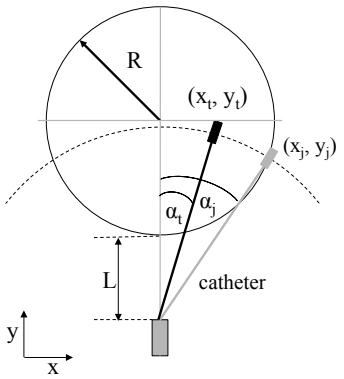

Fig. 7. The catheter tip coordinates x_t, y_t are visually tracked with a blob tracker. The intersection points between the targeted circular path and a circle around the anchor point with radius l_t are derived. Target point (x_j, y_j) is chosen from the two solutions with a flag defining the side of the circle. The desired α_j is calculated from the kinematics model.

which detects the current position (x_t, y_t) of the catheter. The anchor point of the catheter is set by the user prior to execution. The longitudinal direction of the catheter is governed by the PEA that executes a predefined path, as simulated in MATLAB and processed by LabView. Due to catheter stiffness an offset between catheter deflection and field orientation is anticipated, therefore the controlled parameter is the catheter deflection. The catheter moves a distance L in longitudinal direction with initial orientation α_0. Model based closed loop control of the catheter tip orientation is triggered when the currently tracked tip position reaches the targeted circular path with center $\mathbf{C} = (x_C, y_C)$, defined by $(x_j - x_C)^2 + (y_j - y_C)^2 = R^2$. The desired deflection of the catheter tip is dependent on the tracked length $l_t = \sqrt{x_t^2 + y_t^2}$ of the catheter. A circle with radius l_t is described around the anchor point $\mathbf{A} = (x_A, y_A)$ for each l_t as $(x_t - x_A)^2 + (y_t - y_A)^2 = l_t^2$. The intersection point of the two circles defines the targeted point (x_j, y_j) and therefore allows to derive the desired deflection angle α_j from the kinematics model, as illustrated in Figure 7. The targeted point on the circle (x_j, y_j) is chosen from two solutions by evaluating a flag that specifies the side of the targeted circular path. The error between the tracked angle α_t and the desired angle α_j is $\varepsilon_\alpha = \alpha_j - \alpha_t$ which is used to compute a scalable gain factor that adapts the angle of the magnetic field to guide the catheter tip along the circular segment with radius l_t towards the desired point on the targeted circular path with radius R.

IV. RESULTS AND DISCUSSION

A. System Characterization

The maximum torque that can be applied by the catheter tip in the OctoMag workspace is directly obtained from the knowledge of the maximum magnetic field strength (40 mT) and the total magnetization of the three magnets inside the magnetic tool to be 0.0212 mNm. The maximum pushing force that the catheter tip can apply on the material is given by the applied magnetic gradient (1 T/m) and is derived to be 0.529 mN. Catheter bending characteristics are analyzed in relation to field orientation at field magnitudes 10 mT, 20 mT, 30 mT and 40 mT. Figure 8 shows an offset between the orientation of the applied magnetic field and the deflection angle of the catheter. The factor responsible for the large offset is dominated by material stiffness. The graph shows a linear relation between the applied field orientation and the resulting catheter deflection. Thus, a constant gain g_α is implemented to correct for the offset between desired and tracked angles of the catheter. In order to account for small positional errors in real time, a scalable gain factor g_ε is added that is proportional to the error ε_α. Hence, the applied field orientation ψ_{app} is given by $\psi_{app} = g_\alpha \cdot \alpha_t + g_\varepsilon \cdot \varepsilon_\alpha$.

B. Catheter Motion Control

The magnetic catheter and vision based control are tested in an aqueous environment *in vitro* at magnetic field strength of 20 mT. The catheter is attached to the PEA and is guided into the OctoMag workspace through a small tube, the anchor shaft, into a petri-dish filled with distilled water. Results are presented in Figures 9 and 10. Figure 9a) shows the images displayed during control of the catheter tip. The left image is a frame of a realtime video of the catheter in its liquid environment overlaid with a sketch that illustrates the magnitude of current in the eight electromagnets of the OctoMag. The right image shows the tracked position of the catheter tip and the desired circular path. Hybrid

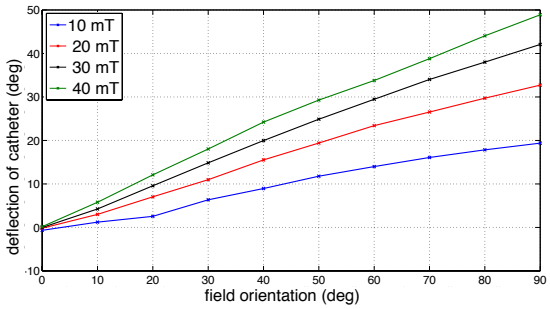

Fig. 8. The catheter deflection angle [°] is graphed at applied magnetic field orientations [°] for field strengths 10 mT, 20 mT, 30 mT and 40 mT. Experiments were done in distilled water.

(a)

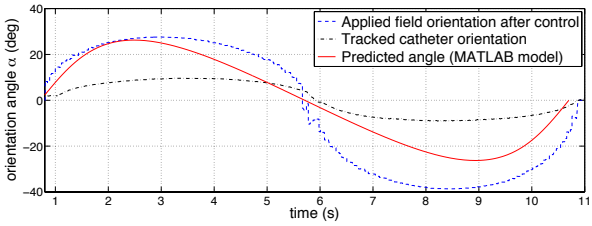

(b)

Fig. 9. a) The displayed images show the catheter tip being controlled by the OctoMag. The currents in the eight electromagnetic coils are imaged in the upper left corner of the displayed image. A second image shows the targeted circular path and the tracked catheter tip. b) The graph shows the angle of the magnetic field after control applied by the OctoMag (blue), the current tracked orientation of the tip α_t (black) and the angle derived in the kinematics model (red). All angles are given in [°].

magnetic-mechanical actuation of a magnetic catheter tip results in circular and continuous motion of the tip with a defined centre location, as seen in Figure 10, where the tracked position of the catheter tip is shown for 20 individual experiments and the black circle defines the targeted path. Figure 9b) illustrates the desired angle of the catheter tip as simulated in MATLAB, the currently tracked tip orientation and the angle of the applied magnetic field after closed loop control. The discrepancy between the modeled angle and the tracked catheter orientation is presumably due to the assumption of inflexibility in the model; in practice some degree of bending is observed.

The experiment was repeated 20 times and repeatability and accuracy with which the catheter tip follows the circular path are evaluated. The position error is derived as the radial difference between the desired circle radius and the tracked position at each central angle of the desired circular trajectory, as illustrated in Figure 11. The accuracy is represented by the mean error that is calculated to be 0.136 mm. The repeatability of the trajectories is expressed through the mean standard deviation for each desired point on the circular path, which is given by 0.018 mm. It is concluded that the model based closed loop control allows for high reproducibility of a trajectory with a mean accuracy of $\pm$ 5.4 % in relation to the circle radius R. However, the results are affected by image noise and small variations in lighting conditions.

C. Experiments in a Lens Capsule Phantom

A perfect capsulorhexis not only requires defined size, shape and location, but must also allow for a continuous and clean edge. To investigate this ability of the hybrid magnetic-mechanical actuation system, cutting experiments

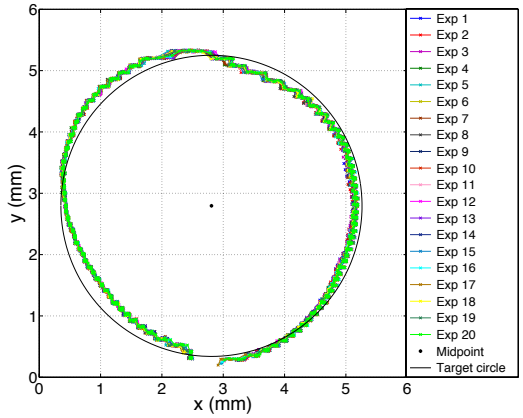

Fig. 10. The graph shows the tracked position in 20 individual experiments and the targeted circular path (black) with radius R =5 mm.

are conducted in agarose, which serves as a capsular lens phantom. In these experiments the magnetic field is applied with a magnitude 20 mT, such that the pitch angle of the catheter tip is set to 40° for deeper penetration of the material and an additional magnetic gradient of 500 mT/m pulls the tip downwards. Hence, an estimated vertical force of 0.170 mN and an additional torque of 0.0081 mNm are applied to the agarose. After performing capsulorhexis in the lens capsule phantom, the agarose is stained with Rhodamine B for better visualization of the edge. A microscope image of a segment of a circular cut is illustrated in Figure 12, the overlaid dashed circle has a diameter of 5 mm. The cut is clearly silhouetted against the lens capsule phantom and exhibits the desired size of 5 mm. Each procedure has a duration time of 10 s which is considerably less than the 2 – 3 min an experienced and well trained surgeon takes for a single capsulorhexis.

V. CONCLUSION

This paper successfully demonstrates automated motion control for capsulorhexis in a capsular lens phantom based on hybrid magnetic-mechanical actuation of a flexible catheter. The longitudinal direction of the catheter is governed by a linear piezoelectric actuator, while the orientation of the

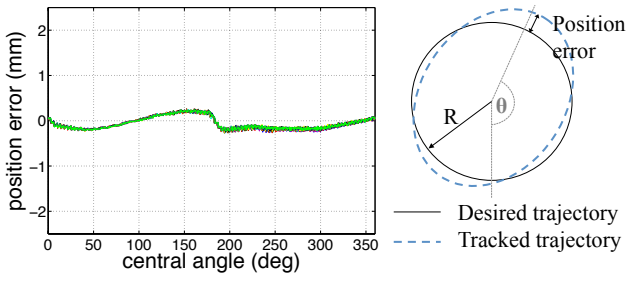

Fig. 11. The position error [mm] is defined as the difference between the desired and the tracked trajectory as shown in the sketch. It is illustrated for 20 individual experiments with a mean error of 0.136 mm and a mean standard deviation of 0.018 mm.

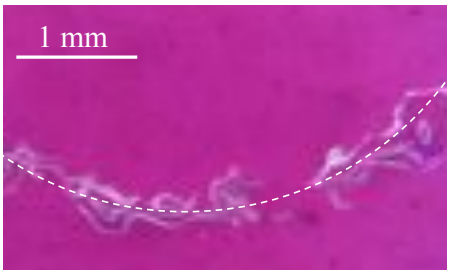

Fig. 12. Segment of a circular cut with diameter 5 mm in agarose as a capsular lens phantom. The dashed circle segment has a radius of 2.5 mm.

catheter tip is controlled by the electromagnetic manipulation system OctoMag. Vision based closed loop control is implemented and guides the bent needle at the tip of a flexible catheter along a continuous circular path with high repeatability. Furthermore, the size and location of the capsulorhexis can be predefined by the user. The demonstrated application of a magnetically oriented catheter is fully automated and shows reproducible results within short duration time, thus, indicating the potential for fast and safe ophthalmic application that potentially does not require excessive medical training. Especially in the underdeveloped world, where a lack of access to ophthalmic surgeons exists, automated capsulorhexis could assist less skilled operators to perform surgery.

A first catheter-based ophthalmic application of the OctoMag is presented in the anterior segment of the eye, demonstrating the versatility of this electromagnetic manipulation system in combination with a mechanical actuator. Flexible catheters with magnetic tips are promising tools to assist in minimally invasive capsulorhexis, especially when a predefined path needs to be followed in a continuous movement with high repeatability. Future work will target the implementation of catheter stiffness in the kinematic model and the model based closed loop control to increase accuracy. Furthermore, the performance of the system will be tested in *ex vivo* experiments. Eventually, results of automated capsulorhexis based on hybrid magnetic-mechanical actuation will be compared to capsulorhexis done manually by ophthalmic surgeons.

ACKNOWLEDGMENT

The authors would like to thank Dr. Katja Ullrich from The Royal Adelaide Hospital for helpful comments on cataract and capsulorhexis. Thanks also goes to Janis Edelmann, Anandeshwar Singh and Taylor Newton for their ideas and help with software and hardware. This work was supported by the European Research Council Advanced Grant BOTMED.

REFERENCES

[1] World Health Organization (WHO), "Priority eye diseases", available at: http://www.who.int/blindness/causes/priority/en/index1.html, accessed: 7.8.2013.

[2] National Eye Institute (NEI), "2010 U.S. Age-Specific Prevalence Rates for Cataract by Age, and Race/Ethnicity", available at: http://www.nei.nih.gov/eyedata/cataract.asp#1, accessed: 7.8.2013.

[3] J. Bolger, "How to master capsulorhexis", in Eye, vol. 9, pp. 526-529, 1995.

[4] R. J. Olson et al., "Cataract treatment in the beginning of the 21st century", in American Journal of Ophthalmology, vol. 136(1), pp. 146-154, 2003.

[5] T. Raviv, "The perfectly sized capsulorhexis", in J. Cataract Refract. Surg., vol. 6, pp. 37-41, June 2009.

[6] Ravalico, G., Tognetto, D., Palomba, M., Busatto, P., Baccara, F. (1996), "Capsulorhexis size and posterior capsule opacification" in Journal of Cataract and Refractive Surgery, vol. 22(1), pp. 98-103, January 1996.

[7] P.K. Gupta, P.S. Jensen, E. de Juan Jr , "Surgical Forces and Tactile Perception During Retinal Microsurgery" in Medical Image Computing and Computer-Assisted Intervention-MICCAI99, Springer Berlin Heidelberg, pp. 1218-1225, January 1999.

[8] A.D. Jagtap, C.N. Riviere, "Applied force during vitreoretinal microsurgery with handheld instruments", in Engineering in Medicine and Biology Society, 2004, IEMBS'04. 26th Annual International Conference of the IEEE, pp. 2771 - 2773, September 2004.

[9] D. Bourla et al, "Feasibility study of intraocular robotic surgery with the da Vinci surgical system", in Retina, vol. 28(1), pp. 154-158, 2008.

[10] T. Nakano, N. Sugita, T. Ueta, Y. Tamaki, M. Mitsuishi, "A parallel robot to assist vitreoretinal surgery", in International Journal of Computer Assisted Radiology and Surgery, vol. 4(6), pp.517 - 526, November 2009.

[11] I. Tsui, A. Tsirbas, C.W. Mango, S.D. Schwartz, J.P. Hubschman, "Robotic Surgery in Ophthalmology", InTech, 2010, ch. 10.

[12] A. Uneri, M.A. Balicki, J. Handa, P. Gehlbach, R.H. Taylor, I. Iordachita, "New steady-hand Eye Robot with micro-force sensing for vitreoretinal surgery", in Biomedical Robotics and Biomechatronics (BioRob), 2010 3rd IEEE RAS and EMBS International Conference on , pp.814,819, September 2010.

[13] R.A. MacLachlan, B.C. Becker, J. Cuevas Tabares, G.W. Podnar, L.A. Lobes, C.N. Riviere, "Micron: an actively stabilized handheld tool for microsurgery", in Robotics, IEEE Transactions on, vol. 28(1), pp. 195 - 212, February 2012.

[14] J. Moreno, et al., "Ablation of Atrioventricular Nodal Reentrant Tachycardia Using Remote Magnetic Guidance (Stereotaxis) Requires Lower Temperature and Power Settings Because of Improved Local Contact", Revista Espaola de Cardiologa (English Edition), vol. 62(9), pp. 1001 - 1011, September 2009.

[15] S. Ernst, et al., "Initial Experience With Remote Catheter Ablation Using a Novel Magnetic Navigation System", in Circulation, vol. 109(12), pp. 1472 - 1475, March 2004.

[16] B.L. Nguyen, J.L. Merino, E.S. Gang, "Remote navigation for ablation procedures–A new step forward in the treatment of cardiac arrhythmias", in Eur. J. Cardiol., vol. 6, pp. 50 - 56, August 2010.

[17] Stereotaxis, "Robotic Navigation", available at: http://www.stereotaxis.com, accessed: 4.9.2013

[18] Magnetecs, "Guiding medical technology", available at: http://www.magnetecs.com, accessed: 4.9.2013

[19] Aeon Scientific AG, "Magnetic Catheter Steering System (Cmag)", available at: http://www.aeon-scientific.com, accessed: 4.9.2013

[20] M. Kummer, J. J. Abbott, B. E. Kratochvil, R. Borer, A. Sengul, B. J. Nelson, "OctoMag: An Electromagnetic System for 5-DOF Wireless Micromanipulation", in Proc. of IEEE International Conference on Robotics and Automation (ICRA), May 2010.

[21] C. Bergeles, M. Kummer, B. E. Kratochvil, C. Framme, B. J. Nelson, "Steerable Intravitreal Inserts for Drug Delivery: In Vitro and Ex Vivo Mobility Experiments", Proc. in 14th International Conference on Medical Image Computing and Computer Assisted Intervention (MICCAI 2011), September 2011.

[22] F. Ullrich, C. Bergeles, J. Pokki, O. Ergeneman, S. Erni, G. Chatzipirpiridis, S. Pan, C. Framme, B. J. Nelson, "Mobility experiments with microrobots for minimally invasive intraocular surgery", in Investigative Ophthalmology and Visual Science, vol. 54(4), pp. 2853-63, April 2013.

[23] C. Bergeles, B. E. Kratochvil, B. J. Nelson, "Visually servoing magnetic intraocular microdevices", IEEE Transactions on Robotics, vol. 28(4), pp. 798-809, 2012.

[24] M. Kummer, J. J. Abbott, B. E. Kratochvil, R. Borer, A. Sengul, B. J. Nelson, "OctoMag: An Electromagnetic System for 5-DOF Wireless Micromanipulation", in IEEE Transactions on Robotics, vol. 26(6), pp. 1006 - 1017, September 2010.